Experimental, SOPPA(CCSD), and DFT Analysis of Substituent Effects on NMR $^1J_{CF}$ Coupling Constants in Fluorobenzene Derivatives

Janaina Dantas Vilcachagua,[†] Lucas C. Ducati,[†] Roberto Rittner,[†] Rubén H. Contreras,[‡] and Cláudio F. Tormena*,[†]

[†]Chemistry Institute, State University of Campinas, Caixa Postal 6154, 13084-971 Campinas, SP, Brazil
[‡]Department of Physics, FCEyN, University of Buenos Aires and IFIBA-CONICET, Buenos Aires, Argentina

ABSTRACT: Interesting insight into the electronic molecular structure changes associated with substituent effects on the Fermi contact (FC) and paramagnetic spin−orbit (PSO) terms of $^1J_{CF}$ NMR coupling constants (SSCCs) in o-X-, m-X-, and p-X-fluorobenzenes (X = NH$_2$; NO$_2$) is presented. The formulation of this approach is based on the influence of different conjugative and hyperconjugative interactions on a second-order property, which can be qualitatively predicted if it is known how they affect the main virtual excitations entering into that second-order property. A set of consistent approximations are introduced in order to analyze the behavior of occupied and virtual orbitals, which define some experimental trends for $^1J_{CF}$ spin−spin coupling constants. In addition, DFT hybrid functionals were used, and a similar degree of confidence to compute the $^1J_{CF}$ with those observed for the SOPPA(CCSD) method was obtained. The $^1J_{CF}$ SSCCs for ezetimibe, a commercially fluorinated drug used to reduce cholesterol levels, were measured and DFT-calculated, and the qualitative approach quoted above was applied. As a byproduct, a possible method to determine experimentally a significant PSO contribution to $^1J_{CF}$ SSCCs is discussed.

1. INTRODUCTION

Organic chemists are interested in compounds containing fluorine atoms due mainly to its steric and polar characteristics. Even a single fluorine substituent, placed at a favorable position within a molecule, can have a remarkable effect upon its physical and chemical properties. Discussion on the impact that fluorine has on physical and chemical properties of compounds has appeared in several reviews and textbooks.[1−4] Selectively fluorinated organic molecules currently account for up to 40% of all agrochemicals and 20% of all pharmaceuticals on the market.[2] The importance of fluorine in medicinal chemistry is widely recognized. Indeed, there is an increasing number of drugs available (antidepressant, immunosuppressant, antibacterial, and antiviral drugs, etc) which contain fluorine atoms, particularly within a fluorobenzene system, and their presence is often extremely important.[3] Further to carbon and hydrogen, ^{19}F is probably the most studied nucleus in NMR. The reasons for this are the fluorine nucleus magnetic properties and the importance of molecules containing fluorine. The ^{19}F nucleus has the advantage of 100% natural abundance, spin $I = 1/2$, and a high magnetogyric ratio, about 0.94 times that of ^{1}H.[4]

Spin−spin coupling constants (SSCCs) between ^{19}F and ^{1}H ($^nJ_{HF}$) or ^{13}C ($^nJ_{CF}$) nuclei are highly variable in magnitude but are also highly characteristic of their chemical environment.[1,4] The SSCC is one of the most important sources of molecular information in high resolution NMR spectroscopy, which is an extremely useful tool for describing molecular electronic structures.[5]

First-principle methods like SOPPA(CCSD) [second-order polarization propagator approximation (coupled cluster singles and doubles)][6] and EOM-CCSD (equation of motion-coupled cluster singles and doubles)[7] explicitly include electron correlation effects, which have increased importance for coupling involving the more electronegative atoms.[8] However, the higher level treatment of correlation effects makes EOM-CCSD significantly more expensive computationally and limits its application to relatively small systems and/or those with high molecular symmetry.[9] On the other hand, SOPPA(CCSD) is much more accessible, but it is also expensive in comparison with DFT-based methods.

It is known that SSCCs measured in an isotropic phase are contributed to, within the Ramsey approximation,[10] by four terms, Fermi contact, (FC), paramagnetic spin orbit, (PSO), spin dipolar, (SD), and diamagnetic spin orbit, (DSO), eq 1, where n stands for the number of formal bonds separating the coupling nuclei, N and N′.

$$^nJ_{NN'} = {}^nJ_{NN'}^{FC} + {}^nJ_{NN'}^{PSO} + {}^nJ_{NN'}^{SD} + {}^nJ_{NN'}^{DSO} \qquad (1)$$

The main aim of this work is to analyze in detail how substituent effects (S) on $^1J_{CF}$ SSCCs, S-SSCCs, can provide interesting insight into changes in the electronic structure produced by such substituents in fluorobenzene derivatives. It is known that in these compounds $^1J_{CF}$ SSCCs are contributed to significantly not only by the FC but also by the PSO and SD terms. However, as it is shown below, the FC and PSO terms are more sensitive to substituents than the SD term; for this reason this study is focused in the former two. On the other hand, the DSO term behavior is very well-known[11], and it cannot be expected to change much for the different benzene derivatives studied in this work (Figure 1). This study was carried out by
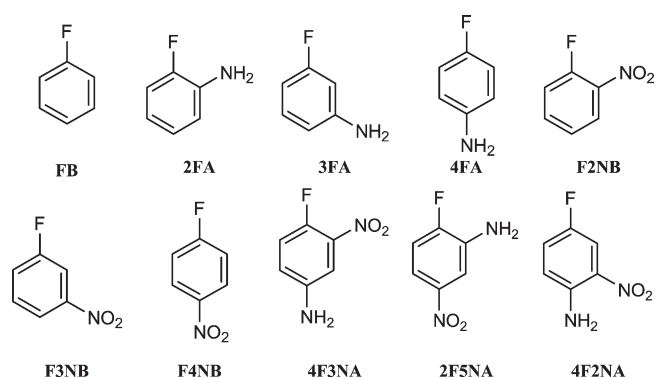
Figure 1. Fluorobenzene derivatives studied in this work. Substituent effects on $^1J_{CF}$ SSCCs are defined by the difference between $^1J_{CF}$ in the X,Y-fluorobenzene derivative and $^1J_{CF}$ SSCC in fluorobenzene (X,Y-S-SSCC). Similar definitions hold for the FC, PSO, SD, and DSO terms.

measuring $^1J_{CF}$ SSCCs in 10 fluorobenzene derivatives and performing their calculations with the SOPPA(CCSD) method. Trends of the influence of conjugative and hyperconjugative interactions on S-SSCCs are based on the FC and PSO expressions obtained within the polarization propagator formalism (PP) at the random phase approximation (RPA).[12] However, it is important to highlight that S-SSCCs are not calculated within the PP formalism at the RPA level of approximation.

Recently, it has been reported that the accuracy of SSCC evaluation correlates with the percentage of exact orbital exchange E_X^{HF} in the functional. The following functionals gave decreasing margins of error: PBE ($E_X^{HF} = 0.0$), B3LYP ($E_X^{HF} = 0.20$), B97-2 ($E_X^{HF} = 0.21$), B97-3 ($E_X^{HF} = 0.27$).[13] Since SSCC SOPPA(CCSD) calculations for larger compounds are computationally demanding, the same calculations quoted above were also carried out within the DFT framework, comparing results for the B3LYP[14] and BHandH[15] functionals with those obtained from SOPPA(CCSD).

Section 2 describes how information about fine details of the electronic molecular structure can be studied resorting to qualitative analyses of SSCC expressions given within the PP formalism taken at the RPA approximation. Experimental and computational details are given in section 3, while results obtained in this work on $^1J_{CF}$ S-SSCCs in compounds shown in Figure 1 are discussed in section 4. In section 4.a, SOPPA-(CCSD) and DFT results are compared, and also a DFT analysis of FC and PSO terms of $^1J_{CF}$ SSCCs for a large fluorinated drug molecule is shown. Finally, some concluding remarks are given in section 5.

2. CONJUGATIVE AND HYPERCONJUGATIVE EFFECTS ON THE FC AND PSO CONTRIBUTIONS TO $^1J_{CF}$ SSCCS

As shown below, the main contributions to the S-SSCC effect on $^1J_{CF}$ SSCCs in compounds studied in this work are those originating in the PSO contribution followed by those originating in the FC term. For this reason this analysis of substituent effects is limited here to these two terms only. It is recalled that a similar approach was applied during the past few years to get insight into different aspects of high resolution NMR parameters.[16]

Briefly, this approach is based on the following grounds. Within the PP approach, all terms of eq 1 can be decomposed into molecular orbital (MO) contributions. Since this study is limited to S-SSCCs on the FC and PSO terms, such MO

decomposition is only shown for them, eq 2, where i and j stand for occupied and a and b for virtual MOs and X stands for either the FC term or the $\alpha\alpha$ diagonal component of the PSO tensor. It is recalled that while the FC term is isotropic, the PSO term is a second-rank tensor.

$$^1J_{CF}^X = \sum_{ia,\,jb} {}^1J_{ia,jb}^X (CF) \qquad (2)$$

2.a. The Fermi Contact Term. Equation 2 for the FC term of $^1J_{CF}$ SSCCs can be written as

$$^1J_{CF}^{FC} = \Omega^{FC} \sum_{ia,\,jb} {}^1J_{ia,jb}^{FC} (CF) \qquad (3)$$

where Ω^{FC} is a constant involving the coupling nuclei magnetogyric ratios as well as universal and numerical constants; its expression is not given explicitly since this a qualitative analysis and therefore it is not affected by a constant. As shown previously[12] MO contributions to the FC term can be written as in eq 4

$$^1J_{ia,jb}^{FC}(C,\,F) = {}^3W_{ia,\,jb}[U_{ia,\,C}^{FC}U_{jb,\,F}^{FC} + U_{ia,\,F}^{FC}U_{jb,\,C}^{FC}] \qquad (4)$$

where $^3W_{ia,jb} = ({}^3A + {}^3B)_{ia,jb}^{-1}$ are the elements of the inverse of the triplet PP matrix, and they involve $i \rightarrow a$ and $j \rightarrow b$ virtual excitations. Matrices ^3A and ^3B are given in terms of bielectronic molecular integrals by

$$^3A_{ia,\,jb} = (\varepsilon_a - \varepsilon_i)\delta_{ab}\delta_{ij} - \langle aj \mid bi \rangle \quad \text{and} \quad {}^3B_{ia,\,jb}$$

$$= \langle aj \mid ji \rangle \quad \text{respectively}$$

with $\langle aj|bi \rangle = \int d^3r_1\,d^3r_2\,a^*(1)j^*(2)(1/r_{12})b(1)i(2)$

In eq 4, $U_{ia,C}^{FC}$ ($U_{jb,F}^{FC}$) are the so-called FC "perturbators", i.e., the matrix elements of the FC operator, between the occupied i (j) and virtual a (b) MOs evaluated at the C (F) site of the coupling nuclei

$$U_{ia,\,N}^{FC} = \langle i|\delta(\vec{r}_N)|a \rangle \qquad (5)$$

where $\delta(\vec{r}_N)$ is Dirac's delta function. The integral in eq 5 yields a measure of the $i \rightarrow a$ and $j \rightarrow b$ virtual excitation strengths owing to the FC operator.

Equations 3, 4, and 5 provide a useful qualitative description of the FC $^1J_{CF}$ S-SSCCs trend along a series of compounds, which could be affected by either the perturbators or the $^3W_{ia,jb}$ term, or both. Using adequate approximations, it is possible to estimate qualitatively how conjugative and/or hyperconjugative interactions affect such S-SSCCs. The approximations are based on the following considerations. Equations 3, 4, and 5 are invariant under unitary transformations; therefore, MOs involved in their expressions can be considered as localized MOs (LMOs). The next approximation is obtained assuming that occupied LMOs behave, under conjugative and hyperconjugative interactions, like core, bonding or lone pair orbitals, while vacant LMOs behave like antibonding or Rydberg orbitals of Weinhold et al.'s[17] NBO approach. ^3W matrix elements are largest for diagonal elements, i.e., those satisfying $i = j$ and $a = b$. The second largest ^3W matrix elements are those "quasi" diagonal; i.e., either occupied or vacant orbitals are equal to each other. Diagonal ^3W matrix elements in eq 4 decrease, in absolute value, whenever there is a hyperconjugative interaction increasing the energy gap between the corresponding a antibonding and the i bonding NBOs, $\varepsilon_a - \varepsilon_i$, and vice versa, hyperconjugative interactions that reduce such gaps, yield an increase, in absolute value, in the

diagonal $^3\mathbf{W}$ element. In a previous paper,[12c] it was studied in detail which are the main three contributions, according to eq 3, to $^1J_{CH}$ SSCCs, i.e., (1) the "bond" contribution, $^1J^B$, where $i = j = \sigma_{CH}$ and $a = b = \sigma^*_{CH}$, which corresponds to a diagonal $^3\mathbf{W}$ matrix element; (2) the "other bond contribution", $^1J^{OB}$, where $i = \sigma_{CH} \neq j$ and $a = b = \sigma^*_{CH}$; and (3) the "other anti-bond contribution", $^1J^{OAB}$, where $i = j = \sigma_{CH}$ and $a = \sigma^*_{CH} \neq b$. While (1) and (3) are positive, (2) is negative. Similarly, for $^1J_{CF}$ SSCC the main four contributions are (1) the "bond" contribution, $^1J^B$, where $i = j = \sigma_{CF}$ and $a = b = \sigma^*_{CF}$, which is positive; (2) the three "lone pair contributions", $^1J^{LP}$, where $i = LP_{1,2,3}(F)$, $a = \sigma^*_{CF}$, which are negative; (3) the "other bond contribution", $^1J^{OB}$, where $i = \sigma_{CC} \neq j = \sigma_{CF}$ and $a = b = \sigma^*_{CF}$, which are negative; and (4) the "other anti-bond contribution", where $i = j = \sigma_{CF}$ and $a = \sigma^*_{CX} \neq b$, which are positive. It should be noted the similitude between $^1J^{OB}$ and $^1J^{LP}$ contributions for $^1J_{CF}$ SSCCs, where their largest difference originates in the larger s % character of the F lone pair deepest in energy compared with those of the "other bonds". Obviously, when one or two of the F three lone pairs is of π symmetry the corresponding $^1J^{OB}$ contribution is null. On the other hand, $LP_1(F)$, which is the LP deepest in energy, has a high s % character. It is observed that $^1J^{LP1}$ contribution does not involve a diagonal $^3\mathbf{W}$ element, and, consequently, it does not depend explicitly on the $\varepsilon_a - \varepsilon_i$ energy gap.

2.b. The Paramagnetic Spin−Orbit Term. For the $PSO^{\alpha\alpha}$ diagonal component contributing to the $^1J_{CF}$ tensor, the expression similar to eq 4[12c] is

$$^1J^{PSO,\alpha\alpha}_{CF} = \Omega^{PSO} \sum_{ia,\,jb} U^{PSO,\,\alpha}_{ia,\,C}{}^1W_{ia,\,jb} U^{PSO,\,\alpha}_{jb,\,F} \qquad (6)$$

where Ω^{PSO} is a constant involving the magnetogyric ratios of the coupling nuclei as well as universal and numerical constants.

The PSO^α perturbators are given in eqs 7a and 7b.

$$U^{PSO,\,\alpha}_{ia,\,F} = \langle i|(\,\vec{r}_F \times \vec{\nabla})_\alpha r_F^{-3}|a\rangle \qquad (7a)$$

and

$$U^{PSO,\,\alpha}_{jb,\,C} = \langle b|(\,\vec{r}_C \times \vec{\nabla})_\alpha r_C^{-3}|i\rangle \qquad (7b)$$

They are equivalent to eq 5 for the FC term.

$^1W_{ia,jb} = (^1A + {}^1B)^{-1}_{ia,jb}$ are the elements of the inverse of the singlet PP matrix, and they involve $i \rightarrow a$ and $j \rightarrow b$ virtual excitations. Matrix $^1\mathbf{A}$ and $^1\mathbf{B}$ elements are given by

$$^1A_{ia,jb} = (\varepsilon_a - \varepsilon_i)\delta_{ab}\delta_{ij} + 2\langle aj \mid ib\rangle - \langle aj \mid bi\rangle \qquad (8)$$

$$^1B_{ia,jb} = \langle ab \mid ji\rangle - 2\langle ab \mid ij\rangle \qquad (9)$$

and the corresponding molecular bielectronic integrals are

$$\langle aj \mid ib\rangle = \int d^3r_1\, d^3r_2\, a^*(1)j^*(2)\frac{1}{r_{12}}b(1)i(2) \qquad (10)$$

Similar approximations to those considered above when analyzing the FC term are now introduced. i, j (a, b) are supposed to be occupied (vacant) LMOs, and their behavior under conjugative and hyperconjugative interactions are assumed to be similar to those of Weinhold et al.'s NBOs.[17] $(\,\vec{r}_F \times \vec{\nabla})_\alpha$ in eq 7a is the 90° rotation operator around the α axis and centered on the F atom. Therefore, a PSO^α perturbator will have a substantial value whenever an occupied LMO rotated 90° around the α axis shows a significant overlap with an antibonding orbital.
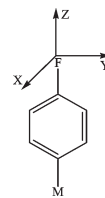

Figure 2. Principal axes for the paramagnetic part of the F nuclear magnetic shielding tensor and for the PSO tensor contribution to $^1J_{CF}$ SSCC (M = H, **FB**; M = NH$_2$, **4FA**; M = NO$_2$, **F4NB** (actually, the NH$_2$ is not planar but this difference is not significant for the PAs orientations when a qualitative description is sought).

The PSO operator in eqs 7a and 7b resembles somewhat that of the paramagnetic part of the nuclear magnetic shielding tensor. This resemblance is analyzed for both quantities in terms of the PP approach. It is also noted that, due to the **4FA**, **FB**, and **F4NB** molecular symmetries, the principal axes (PA) for both the paramagnetic part of the F nuclear magnetic shielding tensor and the PSO tensor of $^1J_{FC}$ SSCC are coincident; they are displayed in Figure 2.

The diagonal terms of the PSO tensor, i.e., the $PSO^{\alpha\alpha}$ contributions to $^1J_{CF}$, are shown in eq 6, where the respective perturbators are given in eq 7, and the diagonal $\sigma^{p,\alpha\alpha}$ component of the paramagnetic part of the F nuclear magnetic shielding tensor within the PP formalism can be written as[18]

$$\sigma^{p,\,\alpha\alpha}(F) = \Omega^\sigma \sum_{ia,\,jb} [U^\alpha_{ia}(^1A + {}^1B)^{-1}_{ia,\,jb} U^\alpha_{jb,\,F}$$
$$+ U^\alpha_{ia,\,F}(^1A + {}^1B)^{-1}_{ia,\,jb} U^\alpha_{jb}] \qquad (11)$$

The Ω^σ factor, which is different from both the Ω^{FC} and Ω^{PSO} factors, involves numerical as well as universal constants. Besides, the respective perturbators are

$$U^{p,\,\alpha}_{ia} = \langle i|(\,\vec{r} \times \vec{\nabla})_\alpha|a\rangle \qquad (12)$$

$$U^\alpha_{ia,\,F} = \langle a|(\,\vec{r}_F \times \vec{\nabla})_\alpha r_F^{-3}|i\rangle \qquad (13)$$

where $\vec{r}$ and $\vec{r}_F$ stand for the electron position vector from the gauge origin and from the F nucleus site, respectively. In this qualitative analysis the gauge origin can be taken at the F nucleus site. In this way, the perturbator of eq 12 can be written as

$$U^{p,\,\alpha}_{ia} = \langle i|(\,\vec{r}_F \times \vec{\nabla})_\alpha|a\rangle \qquad (14)$$

Comparing eq 7a for the α Cartesian component of the PSO^α perturbator with those for the paramagnetic shielding tensor, eqs 13 and 14, it is observed that the former is just equal to eq 7a, while the latter does not contain the r_F^{-3} factor. Within this approximation, the main contributions to eq 11 originate in diagonal terms of the $^1\mathbf{W}$ matrix, which are very sensitive to changes in the respective energy gaps, $\Delta\varepsilon = \varepsilon_a - \varepsilon_i$. However, there is a significant difference between eqs 6 and 11 since both terms of eq 11 for $\sigma^{p,\alpha\alpha}(F)$ are monocentric expressions centered at nucleus F, while eq 6 is a bicentric expression, with the two centers are at the sites of the coupling nuclei. In eq 7a, $\vec{r}_F$ is the electron vector position with origin at the F coupling nucleus, while in eq 7b $\vec{r}_C$ is the electron vector position with origin at the C coupling nucleus.

It is observed that the experimental ^{19}F SCSs, taken from the literature,[19] are linearly correlated to the calculated PSO
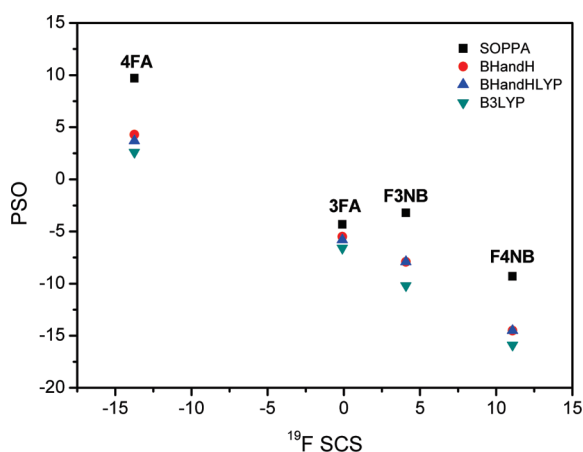
Figure 3. Plot of PSO versus SCS for meta- and para-monosubstituted fluorobenzene derivatives. The linear correlation (R^2), although statistically not very significant since only four points are considered, was calculated for SOPPA(CCSD), BHandH, BHandHLYP, and B3LYP methods obtaining 0.976, 0.997, 0.996, and 0.998, respectively.

S-SSCCs in $^1J_{CF}$ SSCCs in *p*-fluorobenzenes; see Figure 3. Comments made above comparing the operators corresponding to the ^{19}F paramagnetic part of the magnetic shielding constant and that of the PSO term for the $^1J_{CF}$ SSCC suggest that the substituent effect on the PSO perturbator centered at the ^{19}F nucleus, eq 7a, is notably more significant than that centered at the C atom, eq 7b.

3. EXPERIMENTAL AND COMPUTATIONAL DETAILS

3.a. Experimental Section. Compounds studied in this work (Figure 1) are commercially available and were used without further purification. ^1H and $^{13}C\{^1H\}$ NMR spectra were recorded at 25 °C on a Bruker DPX 250 spectrometer, operating at 250 MHz for ^1H and 62.9 MHz for ^{13}C. Samples were prepared as solutions in $CDCl_3$ (30 mg/0.7 mL), and TMS was used as internal reference. Absolute values of $^1J_{CF}$ SSCCs were obtained from $^{13}C\{^1H\}$ NMR spectra. Typical conditions for $^{13}C\{^1H\}$ spectra were 512 transients, spectral width 8 kHz, with 64 k data points, giving an acquisition time of 4.0 s and zero filled to 256 k to give a spectral resolution of 0.2 Hz/point.

3.b. Computational Details. For all compounds quoted in Figure 1 geometries were optimized at the DFT/B3LYP level using the Dunning aug-cc-pVTZ basis set,[20] which includes polarization and diffuse functions. $^1J_{CF}$ SSCCs were calculated using the EPR-III[21] basis set using the following methods: SOPPA(CCSD),[6] the well-known Becke's three-parameter exchange functional, B3LYP,[14] and the Becke's "half and half", BHandH[14c,15] and BHandHLYP functionals,[14,15] the latter includeing 50% HF exchange and 50% Slater exchange. SOPPA(CCSD) calculations were performed using the Dalton 2.0 program package,[22] and DFT calculations were performed using the Gaussian03[23] suite of programs. In the Ramsey approximation[10] the total isotropic SSCCs are expressed as the sum of four contributions, eq 1; all of them were taken into account. The NBO analysis was obtained at the B3LYP/cc-pVTZ level of theory for all studied compounds.

4. RESULTS AND DISCUSSION

In Table 1 are reported the theoretical four isotropic terms of $^1J_{CF}$ SSCC calculated with the SOPPA(CCSD) method and

Table 1. Four Calculated Isotropic Contributions to $^1J_{CF}$ SSCCs at the SOPPA(CCSD) Level and Their Respective S-SSCCs in Compounds 1−10 (Figure 1)^a

compounds	J^{FC}	J^{SD}	J^{PSO}	J^{DSO}	$^1J_{CF}$ calc	$^1J_{CF}$ exp.
FB	−264.2	7.0	0.0	0.8	−256.4	−245.5
S-SSCC	0.0	0.0	0.0	0.0	0.0	0.0
2FA	−258.1	8.6	10.7	0.9	−237.9	−238.4
S-SSCC	6.1	1.6	10.7	0.1	18.5	7.1
3FA	−252.9	6.2	−4.3	0.9	−250.1	−246.2
S-SSCC	+11.3	−0.8	−4.3	0.1	−6.3	−0.7
4FA	−261.7	8.4	9.7	0.9	−242.7	−235.7
S-SSCC	2.7	1.4	9.7	−0.1	13.7	10.5
F2NB	−276.5	2.8	−14.2	1.0	−286.9	−264.8
S-SSCC	11.3	−4.2	−14.2	0.2	20.5	19.3
F3NB	−266.2	5.9	−3.2	0.9	−262.7	−251.2
S-SSCC	−2.0	−1.1	−3.2	0.1	−6.3	−5.7
F4NB	−268.2	4.7	−9.3	0.9	−272.0	−257.9
S-SSCC	−4.0	−2.3	−9.3	−0.1	−15.6	−12.4
4F3NA	−275.6	3.8	−3.1	0.0	−274.9	−255.3
S-SSCC	−11.4	−3,2	−3.1	−0.8	−18.15	−9.8
2F5NA	−266.9	5.8	1.6	0.9	−258.6	−250.1
S-SSCC	−2.7	−1.2	1.6	0.1	−2.2	−4.6
4F2NA	−261.6	7.8	8.3	0.9	−244.6	−239.2
S-SSCC	2.6	0.8	8.3	0.1	11.8	6.3

^{a} Total calculated values are compared with experimental values measured as part of this work. All values are in Hz.

their experimental values measured as part of this work. The respective substituent effects, S-SSCC, on $^1J_{CF}$ SSCCs for fluorobenzene derivatives shown in Figure 1 are also reported. It is observed that, in general, good agreement is found between the experimental and theoretical trends of S-SSCCs, although in some cases the respective quantitative agreement is somewhat poor. However, for **4FA** and **F4NB** that agreement between calculated and observed values is notably better; therefore, the present discussion is started rationalizing para-S-SSCCs. Since it is accepted that the conjugative effect for ortho-substituted compounds is similar to that of para compounds, ortho-S-SSCCs are rationalized in the second place, and finally, meta-S-SSCCs are also rationalized in terms of σ-hyperconjugative interactions.

Since NH_2, and to a lesser extension F, is a resonance electron donor group, while NO_2 is a resonance electron acceptor group, in **4FA** it is expected that NH_2 inhibits to some extent the F resonance effect, while in **F4NB** the NO_2 group is expected to enhance that effect. The largest S-SSCC effects are observed for the FC and PSO terms. For this reason, after a discussion of how the conjugative effect affects the FC and PSO terms of $^1J_{CF}$, the rationalization of those effects will be considered in detail for **2FA**, **3FA**, **4FA**, **FB**, **F2NB**, **F3NB**, and **F4NB** (Figure 1). Calculated parameters necessary to rationalize both types of substituent effects in terms of discussions presented in section 2 are displayed in Table 2. The $LP_3(F) \rightarrow \pi^*$ interactions are employed to gauge the strength of the conjugative interaction between the F atom and the aromatic π system.

A comparison of the $LP_3(F)$ occupancies, displayed in Table 2, shows that the conjugative F effect in **2FA** presents a slightly larger inhibition than in **4FA**. An analogous effect is more evident for **F2NB** and **F4NB**, but in these compounds it corresponds to an increase in the resonance enhancement. Apparently, this

Table 2. Resonance Interaction, σ_{C-F} Bond Length, Energy Gap, and s % Character of σ_{C-F}, LP$_1$(F), LP$_2$(F), and LP$_3$(F) in Compounds 2FA, 3FA, 4FA, FB, F2NB, F3NB, and F4NB[a]

	2FA	3FA	4FA	FB	F2NB	F3NB	F4NB
σ_{C-F} (Å)	1.3622	1.3537	1.3572	1.3527	1.3324	1.3461	1.3437
$\Delta\varepsilon = \varepsilon_{\sigma^*C-F} - \varepsilon_{\sigma C-F}$[b]	1.2462	1.2658	1.2553	1.2667	1.3062	1.2782	1.2862
S-FC	6.1	11.3	2.7	0.0	−11.3	−2.0	−4.0
s % (at F) σ_{C-F}	28.60	29.06	28.70	28.97	29.06	28.89	29.19
s % at LP$_1$(F)	71.36	70.93	71.27	71.00	70.31	71.07	70.78
s % at LP$_2$(F)	0.01	0.00	0.0	0.00	0.60	0.01	0.00
s % at LP$_3$(F)	0.00	0.03	0.0	0.00	0.00	0.00	0.00
S-PSO	10.7	−4.3	9.7	0.0	−14.2	−3.2	−9.3
LP$_2$(F) occupancy	1.9699	1.9714	1.9708	1.9709	1.9662	1.9694	1.9699
LP$_3$(F) occupancy	1.9370	1.9274	1.9347	1.9272	1.9102	1.9233	1.9172

[a] Changes in the resonance interactions are gauged through the occupancy of the respective LP$_3$(F) lone pair. Substituent effects on FC (S-FC) and PSO (S-PSO) terms are also shown. [b] Units of au.

increase in the resonance interaction between substituents placed ortho to each other originates in a proximity effect since in **2FA** the F---H−N distance in the optimized structure is 2.37 Å, while in **F2NB** the similar F---O distance is 2.61 Å. In both cases such distances are shorter than the sum of the respective van der Waals radii, i.e., $(1.47 + 1.20)$ and $(1.47 + 1.52)$ Å, respectively.

In Table 2 it is observed that the inhibition of the F conjugative effect in **4FA** yields a positive increase in both the FC and PSO terms, while the enhancement of the F conjugative effect in **F4NB** renders a negative increase in both terms. These observations are somewhat unexpected since the respective operators describing both interactions are quite different (see section 2). This unexpected behavior is rationalized as follows: an increase (or decrease) in the conjugative effect shortens (or lengthens) the σ_{C-F} bond length. Because S-FC is isotropic, its rationalization is more straightforward than that of S-PSO, and, therefore, it will be considered first. As described in section 2, for the $^1J_{CF}$ SSCCs of compounds considered in Table 2, their main contributions are expected to originate in the diagonal elements of the ^3W matrix $^3W_{\sigma C-F, \sigma^*C-F; \sigma C-F, \sigma^*C-F}$, i.e., the "bond contribution", $^1J^B$, and the main factor affecting it is the corresponding $\Delta\varepsilon = \varepsilon_{\sigma^*C-F} - \varepsilon_{\sigma C-F}$ energy gap. The trend of S-FC for **4FA** and **F4NB** is compatible with this rationalization, and the same assertion holds for **2FA** and **F2NB**. It is noted in both cases that the resonance effect for the ortho position is stronger that for the para position, which can also be observed in the LP$_3$(F) occupancy. Moreover, for meta substituents, the resonance effect is smaller than for substituents either at the ortho or para positions, and the changes observed in the $\Delta\varepsilon = \varepsilon_{\sigma^*C-F} - \varepsilon_{\sigma C-F}$ energy gaps originate both in such differences as well as in the different σ-hyperconjugative interactions of type $\sigma_{C2-C3} \rightarrow \sigma^*_{C1-F}$. In **3FA** the S-FC is larger than expected from the trend observed for the $\Delta\varepsilon = \varepsilon_{\sigma^*C-F} - \varepsilon_{\sigma C-F}$ energy gap, which suggests that the influence of nondiagonal ^3W matrix elements are significant. The most important of them should be $^1J^{LP1(F)}$, which corresponds to a negative contribution and, as explained above, it must be very sensitive to the s % character of the LP$_1$(F). According to Table 2, the **3FA** s % character is smaller than for **2FA** and **4FA**, and the absolute value of $^1J^{LP1(F)}$ should follow the same trend, yielding a larger S-FC, in agreement with its calculated value.

The principal axes (PAs) of the PSO tensor for $^1J_{CF}$ SSCC are X, Y, Z axes shown in Figure 2, for **4FA** and **F4NB**. On the other

hand, assuming that in **3FA** and **F3NB** compounds, the PAs of those corresponding tensors depart only slightly from those shown in Figure 2, and considering that this is only a qualitative analysis, the present approach can also be applied to rationalize the meta S-PSO effects. Tentatively, the same criterion is applied for studying the ortho S-PSO effects.

As commented in Section 2, only nondiagonal elements of the ^1W matrix must be considered for rationalizing the PSO behavior in **2FA, 3FA, 4FA, FB, F2NB, F3NB,** and **F4NB**; therefore, the energy gaps are not relevant for this analysis. Referring to PAs shown in Figure 2, it is observed that the most important perturbators correspond to a 90° rotation around the X axis for LP$_2$(F) and to a 90° rotation around the Y axis for LP$_3$(F). It is noted that such rotations yield PSO principal values of different signs, negative for X and positive for Y. This behavior seems to be the main reason why the calculated PSO term for **FB** is zero, since both components tend to cancel each other.

Since perturbators corresponding to these two PSO$^\alpha$ (PSO^X and PSO^Y) components contain the r_F^{-3} term, their absolute values depend on the s % character of the σ_{C-F} bond at the F atom site, i.e., when increasing that s % character the r_F^{-3} factor, on average, decreases and vice versa. Similar effects originate in the s % character of the LP$_2$(F) and LP$_3$(F) orbitals. According to data collected in Table 2, this rationalization describes correctly the trend of PSO calculated values for **4FA** and for **F4NB**, since for these two compounds the s % character of the LP$_2$(F) and LP$_3$(F) orbitals is 0.00, and the main factors defining the PSO^X and PSO^Y components are, for both of them, the former, the s % character of the σ_{C-F} at F and, for **4FA** the LP$_2$(F) occupancy while for the **F4NB** the LP$_3$(F) occupancy. Changes of the LP$_2$(F) occupancy along the series of compounds, shown in Table 2, are notably smaller than the corresponding changes in the LP$_3$(F) occupancy. Therefore, the comparison of substituent effect on both components, S-PSO^X and S-PSO^Y, can be achieved with some exceptions quoted below, analyzing the LP$_3$(F) occupancy, which corresponds to the negative S-PSO^X component, since its absolute value increases when decreasing that occupancy. This is in agreement with the calculated trend along the series **FB, F4NB, F3NB,** and **F2NB**, where the large absolute value of the latter can be ascribed to the s % character at the LP$_2$(F). The same trend holds for **FB, 4FA,** and **2FA**. The negative value for **3FA** can be rationalized considering the higher σ_{C-F} bond s % character at the site of the F atom.

4.a. Comparison of Calculated $^1J_{CF}$ between SOPPA-(CCSD) and DFT. To verify the applicability of DFT functional to rationalize with confidence $^1J_{CF}$ S-SSCCs, a comparison between SOPPA(CCSD) and DFT calculations was performed. The corresponding SOPPA(CCSD), DFT/BHandH, DFT/BHandHLYP, and DFT/B3LYP values for all four isotropic contributions to SSCC are listed in Table 3 for the following seven compounds (**FB, 2FA, 3FA, 4FA, F2NB, F3NB,** and **F4NB**; Figure 1). They are also compared with the respective experimental values.

The best numerical agreement for $^1J_{FC}$ SSCCs data with experimental values was obtained with SOPPA(CCSD), as known from current literature.[8,9,24] The discrepancy between the experimental and these different DFT levels, especially with B3LYP (Table 3), originates mainly in the FC and PSO terms, which were evaluated considering virtual triplet and singlet transitions, respectively. A poor description of the triplet mechanisms responsible for the Fermi contact and the spin-dipole contributions to the coupling constants seems to be the main reason for this discrepancy.[25−28]

1276

dx.doi.org/10.1021/jp110290b |*J. Phys. Chem. A* 2011, 115, 1272–1279

Table 3. Theoretical and Experimental S-SSCC Values of $^1J_{CF}$ (Hz) Couplings for Fluorobenzene Derivatives at Different Levels of Theory

compound	method	J^{FC}	J^{SD}	J^{PSO}	J^{DSO}	$^1J_{CF}$ calc.	S-SSCC^a	$^1J_{CF}$ exp.
FB	SOPPA(CCSD)	−264.2	7.0	0.0	0.8	−256.4	0	−245.5 (0.0)^b
	BHandH	−269.8	5.1	−4.7	0.9	−268.4	0	
	BHandHLYP	−274.7	3.9	−4.9	0.9	−274.8	0	
	B3LYP	−312.1	6.2	−6.8	0.9	−311.8	0	
2FA	SOPPA(CCSD)	−258.1	8.6	10.7	0.9	−237.9	18.5	−238.4 (7.1)^b
	BHandH	−268.1	7.0	5.3	1.0	−254.8	13.6	
	BHandHLYP	−272.9	5.9	4.7	1.0	−261.3	13.5	
	B3LYP	−309.5	8.3	3.9	1.0	−296.3	15.5	
3FA	SOPPA(CCSD)	−252.9	6.2	−4.3	0.9	−250.1	6.3	−246.2 (−0.7)^b
	BHandH	−267.6	5.6	−5.5	0.9	−266.5	1.9	
	BHandHLYP	−272.0	4.6	−5.8	0.9	−272.3	2.5	
	B3LYP	−308.9	6.6	−6.6	0.9	−308.0	3.8	
4FA	SOPPA(CCSD)	−261.7	8.4	9.7	0.9	−242.7	13.7	−235.7 (9.6)^b
	BHandH	−267.3	6.5	4.3	0.9	−255.6	12.8	
	BHandHlyp	−272.2	5.3	3.7	0.9	−262.3	12.5	
	B3LYP	−309.8	7.8	2.6	0.9	−298.5	13.3	
F2NB	SOPPA(CCSD)	−276.5	2.8	−14.2	1.0	−286.9	−30.5	−264.8 (−5.7)^b
	BHandH	−280.7	0.3	−19.4	1.0	−298.8	−30.4	
	BHandHLYP	−287.2	−1.3	−19.5	1.0	−307.0	−32.2	
	B3LYP	−321.4	1.6	−20.6	1.0	−339.4	−27.6	
F3NB	SOPPA(CCSD)	−266.2	5.9	−3.2	0.9	−262.7	−6.3	−251.2 (−5.7)^b
	BHandH	−270.7	3.9	−7.9	0.9	−273.8	−5.4	
	BHandHLYP	−275.9	2.6	−7.9	0.9	−280.3	−5.5	
	B3LYP	−313.1	5.1	−10.2	0.9	−317.3	−5.5	
F4NB	SOPPA(CCSD)	−268.2	4.7	−9.3	0.9	−272.0	−15.6	−257.9 (−12,4)^b
	BHandH	−272.4	2.3	−14.5	0.9	−283.8	−15.4	
	BHandHLYP	−277.7	0.9	−14.5	0.9	−290.4	−15.6	
	B3LYP	−313.8	3.6	−15.9	0.9	−325.2	−13.4	

^{a} S-SSCC = $^1J_{CF}$ calc. for substituted fluorobenzene − $^1J_{CF}$ calc. for fluorobenzene. ^{b} Experimental S-SSCC.

The DFT/BHandH is also a hybrid functional, which includes an ad hoc mixture of half the exact (HF) exchange with half of the uniform electron gas exchange, plus Lee, Yang, and Parr's expression for correlation energy. It provided better results than B3LYP and BHandHLYP functionals. Therefore, it was suggested[29] that an adequate exchange functional (BHandH: $(E_X^{HF} = 0.5)/(E_X^{LSDA} = 0.5)$, in comparison with B3LYP: $(E_X^{HF} = 0.2)/(E_X^{LSDA} = 0.8)$), should improve the accuracy of the DFT calculations in predicting the spin-density in such complex structures. The deficiencies have been attributed to self-interaction errors[6a] in pure (approximate) density functionals. The increase of Hartree−Fock exchange leads, in some cases, to an improvement in the numerical results.[25] The calculated value for $^1J_{CF}$ = −274.7 Hz in fluorobenzene obtained by BHandHLYP (version of B3LYP functional, using 50% E_X^{HF} and 50% E_X^{LSDA}) leads to a better agreement for these SSCC values in comparison to experimental data (Table 3). This fact reinforces the importance of E_X^{HF} in the density functional in order to obtain a better accuracy in SSCC calculations involving lone pair bearing atoms.

In Table 3 it is observed that S-SSCCs calculated at different levels yield the same trend, and they compare favorably with the experimental values with the exception of ortho-substituted compounds. In fact, for **2FA** and especially for **F2NB** calculated S-SSCCs show absolute values notably larger for calculated than

Scheme 1. Ezetimibe Molecule
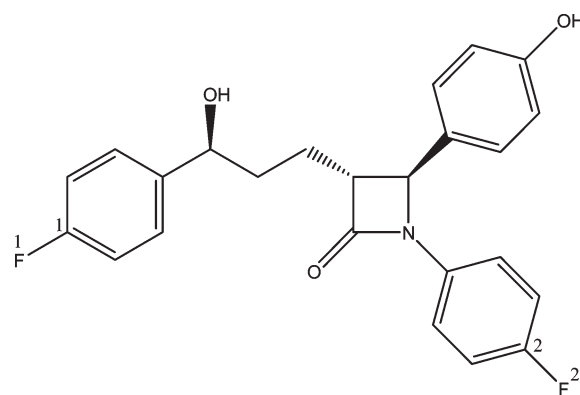
for experimental data, although the respective signs are in agreement. However, it is important to highlight that S-SSCCs calculated with different approaches are similar enough to suggest that those DFT functionals can be used with reasonable confidence to perform similar analyses to those shown above for fluorobenzene derivatives for larger molecular systems like ezetimibe, which is a drug used to reduce the cholesterol blood level by decreasing cholesterol absorption in the intestine

1277

dx.doi.org/10.1021/jp110290b |*J. Phys. Chem. A* 2011, 115, 1272–1279

Table 4. Experimental and Theoretical Values of $^1J_{C1F1}$ and $^1J_{C2F2}$ SSCCs for Ezetimibe^a

$^1J_{CF}$	J^{FC}	J^{SD}	J^{PSO}	J^{DSO}	$^1J_{CF}$ calc.	$^1J_{CF}$ exp.
$^1J_{C1F1}$	−269.9	4.5	−6.0	0.9	−270.4	−246.1
FB	−269.8	5.1	−4.7	0.9	−268.4	−245.5
$^1J_{C2F2}$	−258.4	5.1	−1.5	0.9	−264.0	−243.9

^{a} The different terms are compared with those in fluorobenzene (FB). All theoretical values were obtained at the BHandH/EPR-III level and are given in Hz.

Table 5. Resonance Interaction, σ_{C-F} Bond Length, Energy Gap, and s % Character of σ_{C-F}, $LP_1(F)$, $LP_2(F)$, and $LP_3(F)$ in F_1 and F_2 for Ezetimibe and Those in FB^a

	$^1J_{C1F1}$	$^1J_{CF}$(**FB**)	$^1J_{C2F2}$
σ_{C-F} (Å)	1.3489	1.3527	1.3514
$\Delta\varepsilon = \varepsilon_{\sigma^*C-F} - \varepsilon_{\sigma C-F}{}^b$	1.2756	1.2667	1.2697
S-FC	−0.1	0.0	11.4
s % (at F) σ_{C-F}	29.15	28.97	29.01
s % at $LP_1(F)$	70.96	71.00	70.82
s % at $LP_2(F)$	0.00	0.00	0.0
s % at $LP_3(F)$	0.00	0.00	0.00
S-PSO	−1.3	0.00	3.2
$LP_2(F)$ occupancy	1.9704	1.9709	1.9704
$LP_3(F)$ occupancy	1.9259	1.9272	1.9294

^{a} Changes in the resonance interactions are gauged through the occupancy of the respective $LP_3(F)$ lone pair. Substituent effects on FC (S-FC) and PSO (S-PSO) terms are also shown. ^{b} In au.

(Scheme 1). This compound contains two different fluorinated aromatic rings, where the analysis shown above is applied.

Theoretical $^1J_{CF}$ SSCCs for ezetimibe were calculated using the DFT/BHandH functional. Here, it is stressed that SOPPA-(CCSD) calculations can not be carried out due to the large size of this molecular system. The experimental and theoretical values for $^1J_{CF}$ SSCCs for ezetimibe are shown in Table 4, where they are also compared with the respective values in **FB**.

Taking $^1J_{CF}$ for fluorobenzene as reference (Table 4), it can be observed a slightly negative increase for $^1J_{C1F1}$ and a positive increase for $^1J_{C2F2}$. However, it is noted that FCs for the former coupling differ only 0.1 Hz from that in **FB**. On the other hand, for the latter the FC and PSO terms define its trend. These two observations suggest that a similar analysis performed for fluorobenzene derivatives can be used for the ezetimibe molecule. To this end, all parameters necessary to rationalize the FC and PSO behavior are collected in Table 5 (see Table 2). It is noted that a comparison of this type amounts to assume that the PA axes for the **PSO** contribution are similarly oriented like in Figure 2.

Further comments can be made on data displayed in Table 5. The negligible FC S-SSCC in $^1J_{C1F1}$ can be rationalized as a compensation of the following two effects; the larger $\Delta\varepsilon_1$ energy gap in comparison to **FB** yields a decrease in $^1J^B{}_1$, while the increase in the s % character of the σ_{C1-F1} at the F_1 atom yields an increase in the same term. The $^1J_{C2F2}$ trend is rationalized on the following grounds: the energy gap $\Delta\varepsilon_2$ yields a slight decrease in $^1J^B{}_2$ which is mostly compensated by the also slight increase in the s % character of the σ_{C2-F2} at the F_2 atom. Apparently, the calculated trend is mainly determined by the lower s % character at $LP_1(F2)$, which reduces the negative $^1J[LP2(F2)]$ contribution.

The trends of the PSO^α component can be compared with that on benzene. As commented above, the X component is negative while the Y is positive. The former corresponds to a 90° rotation of LP_2 around the X axis, while the latter corresponds to a 90° rotation of LP_3 around the Y axis. According to the occupancies of LP_2 and of LP_3, it is observed that the former is practically the same for $^1J_{C1F1}$, $^1J_{C2F2}$, and $^1J_{CF}$(**FB**). Therefore, the differences observed for these three PSO terms are originated in the LP_3 contribution. In fact, such occupancies suggest that PSO^Y increases for $^1J_{C2F2}$ and decreases for $^1J_{C1F1}$ in agreement with the calculated values displayed in Table 5.

Based on the $LP_3(F)$ occupancy, it is noted that in ezetimibe while the F_1 atom undergoes a stronger conjugative interaction than that in **FB**, the F_2 conjugative interaction is weaker than that in **FB**. In para position with respect to F_2, there is a three-coordinated N atom and it causes an inhibition of the F resonance interaction, which is notably smaller than for the amino group in **4FA**. The rationalization of this behavior seems to originate in this fact, the N atom in ezetimibe is placed α to a carbonyl group, and the following calculated interactions are worth mentioning: $LP_1(N) \rightarrow \pi^*_{C=O} = 58.6$ kcal/mol while $LP_1(N) \rightarrow \pi^*_{C=C} = 36.6$ kcal/mol. The latter should be compared with $LP_1(N) \rightarrow \pi^*_{C=C} = 25.7$ kcal/mol in **4FA**. As a result, in ezetimibe the F_2 resonance interaction is notably more inhibited than in **4FA** (Table 2).

5. CONCLUSIONS

A qualitative approach, which allows one obtaining an in-depth insight into electronic molecular structure changes along a series of compounds by studying high resolution NMR parameters, was presented in previous papers.[12] In this work such an approach is applied to rationalize several substituent effects on the FC and PSO contributions to $^1J_{FC}$ S-SSCCs in terms of changes in the molecular electronic structure. First, it is applied to analyze those SSCC terms in monosubstituted fluorobenzenes. Those analyses were complemented, on one hand, with measurements of their experimental values for the compounds shown in Table 1 and, on the other hand, with high level ab initio calculations, carried out within the SOPPA(CCSD) method. In this way, very interesting para, meta, and ortho substituent effects on $^1J_{CF}$ SSCC rationalizations were obtained. The following results are highlighted.

Para and meta S-PSO SSCCs were observed to approximately correlate linearly with the corresponding fluorine SCSs (taken from the literature). Such correlation was ascribed to the close resemblance between the operators describing the paramagnetic part of the fluorine nuclear magnetic shielding tensor and the part of the PSO operator centered at the F atom. This suggests an approximate test to verify experimentally, if a given $^1J_{CF}$ SSCC in a series of compounds shows significant S-PSO can be obtained, by observing the corresponding fluorine SCSs in the same series of compounds. It is recalled that, for the time being, no experimental approach can be used to estimate the presence of the PSO term in a given SSCC.

Ortho S-PSO studied in this work provided an interesting description of the proximity contribution to the so-called "ortho" substituent effect. The description given many years ago by Lee and Chesnut[30] for the proximity effect between two moieties on nuclear magnetic shielding constants is now described in terms of changes in the LMOs representing the fluorine lone pairs.

For the application of this approach to larger compounds, S-SSCCs calculated within the DFT framework employing three different functionals were compared with those obtained with the SOPPA(CCSD) method, for some model compounds. Since a good agreement was found for S-SSCCs, the molecular electronic structure that yields both $^1J_{CF}$ SSCCs in ezetimibe could be compared. Results thus obtained show that this qualitative approach can be successfully used to study larger compounds using moderate computational resources.

■ AUTHOR INFORMATION

Corresponding Author

*E-mail tormena@iqm.unicamp.br.

■ ACKNOWLEDGMENT

■ REFERENCES

(1) (a) Michalik, M.; Hein, M.; Frank, M. *Carbohydr. Res.* **2000**, *327*, 185–218. (b) O'Hagan, D. *Chem. Soc. Rev.* **2008**, *37*, 308.

(2) Grushin, V. *Acc. Chem. Res.* **2010**, *43*, 160.

(3) (a) Purser, S.; Moore, P. R.; Swallow, S.; Gouverneur, V. *Chem. Soc. Rev.* **2008**, *37*, 320. (b) Kirk, K. L. *J. Fluorine Chem.* **2006**, *127*, 1013.

(4) (a) Dolbier Jr., W. R. *Guide to Fluorine NMR for Organic Chemists*; Wiley-VCH: Darmstadt, Germany, 2009;(b) Hagmann, W. K. *J. Med. Chem.* **2008**, *51*, 4359.

(5) (a) Helgaker, T.; Pecul, M. In *Calculation of NMR and EPR Parameters, Theory and Application*; Kaupp, M., Buhl, M., Malkin, V. G., Eds.; Wiley-VCH Verlag: Weinheim, Germany, 2004; Chapter 7, p 101. (b) Malkina, O. L. In *Calculation of NMR and EPR Parameters, Theory and Application*; Kaupp, M., Buhl, M., Malkin, V. G., Eds.; Wiley-VCH Verlag: Weinheim, Germany, 2004; Chapter 19, p 307.

(6) (a) Enevoldsen, T.; Oddershede, J.; Sauer, S. P. A. *Theor. Chem. Acc.* **1998**, *100*, 275. (b) Sauer, S. P. A. *J. Phys. B: At., Mol. Opt. Phys.* **1997**, *30*, 3773.

(7) (a) Koch, H.; Jørgensen, P. *J. Chem. Phys.* **1990**, *93*, 3333. (b) Stanton, J. F.; Bartlett, R. J. *J. Chem. Phys.* **1993**, *98*, 7029. (c) Koch, H.; Kobayashi, R.; Sánchez de Merás, A.; Jørgensen, P. *J. Chem. Phys.* **1994**, *100*, 4393. (d) Kállay, M.; Gauss, J. *J. Chem. Phys.* **2004**, *121*, 9257.

(8) Del Bene, J. E.; Provasi, P. F.; Alkorta, I.; Elguero, J. *Magn. Reson. Chem.* **2008**, *46*, 1003.

(9) Del Bene, J. E.; Alkorta, I.; Elguero, J. *J. Chem. Theor. Comp.* **2009**, *5*, 208.

(10) (a) Ramsey, N. F.; Purcell, E. M. *Phys. Rev.* **1952**, *85*, 143. (b) Ramsey, N. F. *Phys. Rev.* **1953**, *91*, 303.

(11) Perez, J. E; Ortiz, F. S.; Contreras, R. H.; Giribet, C. G.; Ruiz de Azúa, M. C. *J. Mol. Struct. (Theochem)* **1990**, *210*, 193.

(12) (a) Oddershede, J. Polarization Propagator Calculations. In *Advances in Quantum Chemistry*; Löwdin, P.-O., Ed.; Elsevier: New York, 1978; Vol. 11, p 272.(b) Diz, A. C.; Giribet, C. G.; Ruiz de Azúa, M. C.; Contreras, R. H. *Int. J. Quantum Chem.* **1990**, *37*, 663. (c) Contreras, R. H.; Ruiz de Azúa, M. C.; Giribet, C. G.; Aucar, G. A.; Lobayan de Bonczok, R. *J. Mol. Struct. (Theochem)* **1993**, *284*, 249. (d) Giribet, C. G.; Ruiz de Azúa, M. C.; Contreras, R. H.; Lobayan de Bonczok, R.; Aucar, G. A.; Gomez, S. *J. Mol. Struct. (Theochem)* **1993**, *300*, 467.

(13) (a) Patchkovskii, S.; Autscgbach, J.; Ziegler, T. *J. Chem. Phys.* **2009**, *115*, 26. (b) Keal, T. W.; Helgaker, T.; Salek, P.; Tozer, D. J. *Chem. Phys. Lett.* **2006**, *425*, 163.

(14) (a) Becke, A. D. *Phys. Rev.* **1988**, *A 38*, 3098. (b) Lee, C.; Yang, W.; Parr, R. G. *Phys. Rev.* **1988**, *B 37*, 785. (c) Becke, A. D. *J. Chem. Phys.* **1993**, *98*, 5648.

(15) (a) Becke, A. D. *J. Chem. Phys.* **1993**, *98*, 1372. (b) Peréz-Jordá, J. M.; Becke, A. D. *Chem. Phys. Lett.* **1995**, *233*, 134.

(16) (a) Barone, B.; Contreras, R. H.; Díez, E.; Esteban, A. L. *Mol. Phys.* **2003**, *101*, 1297. (b) Barone, V.; Provasi, P. F.; Peralta, J. E.; Snyder, J. P.; Stephan, P. A.; Sauer, S. P. A.; Contreras, R. H. *J. Phys. Chem. A* **2003**, *107*, 4748. (c) Contreras, R. H.; Esteban, A. L.; Díez, E.; Della, E. W.; Lochert, I. J.; dos Santos, F. P.; Tormena, C. F. *J. Phys. Chem. A* **2006**, *110*, 4266. (d) Esteban, A. L.; Díez, E.; Della, E. W.; Ian J. Lochert, I. J.; dos Santos, F. P.; Tormena, C. F. *J. Phys. Chem. A* **2006**, *110*, 4266. (e) Cunha Neto, A.; Ducati, L. C.; Rittner, R.; Tormena, C. F.; Contreras, R. H.; Frenking, G. *J. Chem. Theory Comp.* **2009**, *5*, 2222. (f) Contreras, R. H.; Llorente, T.; Pagola, G. I.; Bustamante, M. G.; Pasqualini, E. E.; Melo, J. I.; Tormena, C. F. *J. Phys. Chem. A* **2009**, *113*, 9874. Contreras, R. H.; Gotelli, G.; Ducati, L. C.; Barbosa, T. M.; Tormena, C. F. *J. Phys. Chem. A* **2010**, *114*, 1044.

(17) (a) Reed, A. E.; Curtiss, L. A.; Weinhold, F. *Chem. Rev.* **1988**, *88*, 899.(b) Weinhold, F. In *Encyclopedia of Computational Chemistry*; Schleyer, P. v. R., Ed.; Wiley: New York, 1998; Vol. 3, p 1792.

(18) Contreras, R. H.; Giribet, C. G.; Ruiz de Azúa, M. C.; Ferraro, M. B. Electronic origin of high resolution NMR parameters. In *Computational Chemistry: Structure, Interactions and Reactivity*; Fraga, S., Ed.; *Studies in Physical and Theoretical Chemistry*; Elsevier Science Publishers B.V: New York, 1992; Vol. 77B, p 212.

(19) Fifolt, M. J.; Soyka, S. A.; Roger, R. A.; Hojnicki, D. S. *J. Org. Chem.* **1989**, *54*, 3019.

(20) (A) Dunning, T. H., Jr. *J. Chem. Phys.* **1989**, *90*, 1007. (b) Kendall, R. A.; Dunning, T. H., Jr.; Harrison, R. J. *J. Chem. Phys.* **1992**, *96*, 6769.

(21) Barone, V. *J. Chem. Phys.* **1994**, *101*, 6834.

(22) DALTON, a molecular electronic structure program, Release 2.0 (2005). Available from http://www.kjemi.uio.no/software/dalton/dalton.html

(23) Frisch, M. J.; Trucks, G. W.; Schlegel, H. B.; Scuseria, G. E.; Robb, M. A.; Cheeseman, J. R.; Montgomery, J. A., Jr.; Vreven, T.; Kudin, K. N.; Burant, J. C.; Millam, J. M.; Iyengar, S. S.; Tomasi, J.; Barone, V.; Mennucci, B.; Cossi, M.; Scalmani, G.; Rega, N.; Petersson, G. A.; Nakatsuji, H.; Hada, M.; Ehara, M.; Toyota, K.; Fukuda, R.; Hasegawa, J.; Ishida, M.; Nakajima, T.; Honda, Y.; Kitao, O.; Nakai, H.; Klene, M.; Li, X.; Knox, J. E.; Hratchian, H. P.; Cross, J. B.; Bakken, V.; Adamo, C.; Jaramillo, J.; Gomperts, R.; Stratmann, R. E.; Yazyev, O.; Austin, A. J.; Cammi, R.; Pomelli, C.; Ochterski, J. W.; Ayala, P. Y.; Morokuma, K.; Voth, G. A.; Salvador, P.; Dannenberg, J. J.; Zakrzewski, V. G.; Dapprich, S.; Daniels, A. D.; Strain, M. C.; Farkas, O.; Malick, D. K.; Rabuck, A. D.; Raghavachari, K.; Foresman, J. B.; Ortiz, J. V.; Cui, Q.; Baboul, A. G.; Clifford, S.; Cioslowski, J.; Stefanov, B. B.; Liu, G.; Liashenko, A.; Piskorz, P.; Komaromi, I.; Martin, R. L.; Fox, D. J.; Keith, T.; Al-Laham, M. A.; Peng, C. Y.; Nanayakkara, A.; Challacombe, M.; Gill, P. M. W.; Johnson, B.; Chen, W.; Wong, M. W.; Gonzalez, C.; Pople, J. A. *Gaussian 03*, Revision E.01; Gaussian, Inc.: Wallingford, CT, 2004.

(24) Alkorta, I.; Blanco, F.; Elguero, J. *J. Mol. Struct.* **2010**, *964*, 119.

(25) Keal, T. W.; Tozer, D. J. *J. Chem. Phys.* **2003**, *119*, 3015.

(26) Keal, T. W.; Helgaker, T.; Tozer, D. J. *Chem. Phys. Lett.* **2004**, *391*, 374.

(27) Keal, W. T.; Helgaker, T.; Salek, P.; Tozer, D. J. *Chem. Phys. Lett.* **2006**, *425*, 163.

(28) Helgaker, T.; Jaszunski, M.; Pecul, M. *Prog. Nucl. Magn. Reson. Spectrosc.* **2008**, *53*, 249.

(29) Lanto, P.; Vaara, J.; Helgaker, T. *J. Chem. Phys.* **2002**, *117*, 5998.

(30) (a) Li, S.; Chesnut, D. B. *Magn. Reson. Chem.* **1985**, *23*, 625. (b) Li, S.; Chesnut, D. B. *Magn. Reson. Chem.* **1986**, *24*, 93.